Quantum chemical investigation of the oxidation reactions of the dinuclear low-valent molybdenum carbonyl complexes containing thiolato bridges

Chunwan Liu*, Huang Tang, Xingru Lin, Botao Zhuang and **Jiaxi Lu**

Fujian Institute of Research on the Structure of Matter, Fuzhou Laboratory of Structural Chemistry, Chinese Academy of Sciences, Fuzhou, Fujian 350002 (China)

(Received July 2, 1990)

Abstract

The electronic structure and bonding of the dinuclear low-valent molybdenum thiolato-bridged complexes, $[Mo_2(\mu\text{-}SR)_2(CO)_8]^{n-}$ ($n=2$, **1**; $n=0$, **2**; $R=CH_2COOEt$), $Mo_2(\mu\text{-}SR)_2(CO)_6(NCCH_3)_2$ (**3**) and $[Mo_2(\mu\text{-}S,S\text{-}C_6H_4\text{-}1,2(CO)_7]^{2-}$ (**4**), have been studied using the EHMO method. On the basis of analysis of the MO energies, orbital characteristics, atomic charges and Mulliken bond orders, the possible oxidation of these complexes was discussed. The Walsh diagram shows that further two-electron oxidation of **2** would be very unlikely. However, because **4** contains a non-planar MoS_2Mo bimetallic core, an irreversible one-electron oxidation in solution could take place to form a monoanion complex $[Mo_2(\mu\text{-}S,S\text{-}C_6H_4\text{-}1,2)(CO)_7(NCH)]^{1-}$.

Introduction

Molybdenum is one of the crucial elements in the active center of nitrogenases. In order to understand possible biological functions of molybdenum in the active centers of nitrogenase, the investigation of redox process and solvent ligand substitution effect in synthetic molybdenum complexes is important. In the past few years, a series of dinuclear low-valent thiolato-bridged molybdenum(0, I) complexes have been synthesized, i.e. $[Et_4N]_2[Mo_2(CO)_8(SR)_2]$ ($R=Ph$, Bu^t, CH_2CO_2Et and $C_6H_5CH_2$) [1–4] and $Mo_2(CO)_{8-n}(SR)_2L_n$ ($R=Ph$, Bu^t, CH_2CO_2Et and $C_6H_5CH_2$; $L=MeCN$, Ph_3P; $n=0$, 2) [5, 6]. Among other things, a new dinuclear Mo(0) carbonyl complex with μ^2-thiolato-bridged $[Et_4N]_2[Mo_2(\mu\text{-}S,S\text{-}C_6H_4\text{-}1,2)(CO)_7]$ has been well-characterized recently, which contains a non-planar MoS_2Mo core adopting the 'butterfly' conformation [7], and the structure and electrochemical property of these complexes have been reported.

In this study, using the EHMO method we have investigated the electronic structure and bonding of four dinuclear low-valent molybdenum complexes, $[Mo_2(\mu\text{-}SR)_2(CO)_8]^{n-}$ ($n=2$, **1**; $n=0$, **2**; $R=CH_2COOEt$), $Mo_2(SR)_2(CO)_6(NCCH_3)_2$ (**3**) and $[Mo_2(\mu\text{-}S,S\text{-}C_6H_4\text{-}1,2)(CO)_7]^{2-}$ (**4**), and discussed their relevance to the redox properties. In the calculations, the original R and CH_3 groups were replaced by H atoms to simplify the systems. The bond lengths of all carbonyl groups in these complexes were taken to be equivalent. The EHMO program and parameters were the same as those used in our previous work [8].

*Author to whom correspondence should be addressed.

Results and discussion

$[Mo_2(\mu\text{-}SH)_2(CO)_8]^{2-}$ (1)

Using the technique of fragment molecular orbital analysis, we consider the orbital interaction between the HS···SH bridge and two $Mo(CO)_4$ fragments. The d–d orbital components of the molecular orbitals (MOs) of the fragment $(CO)_4Mo\text{–}Mo(C)_4$ are listed in Table 1. The orbital components of **1** are listed in Table 2 and the MO correlation diagram is given in Fig. 1.. The occupied frontier orbitals (b_{1u}, a_g, a_u, b_{1g}, b_{2g} and b_{3u}) are contributed markedly from the Mo d orbitals. With the same symmetry (D_{2h}) of **1**, the frontier orbitals of the fragment HS···SH can be classified into the irreducible representation of a_g, b_{2u}, b_{3u}, b_{1u}, b_{1g} and b_{3g}. The results of population analysis reveal that the d–d interaction mainly exists between Mo atoms in **1**, and the Mo d-based MOs (b_{1u}, b_{1g}, a_g and b_{3u}) of the fragment $(CO)_4Mo\cdots Mo(CO)_4$ were split by the orbital in-

0020-1693/91/$3.50

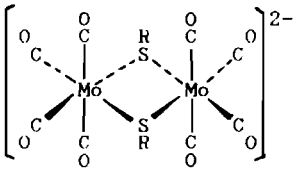

1 (D_{2h})

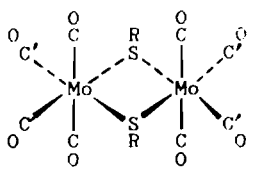

2 (D_{2h})

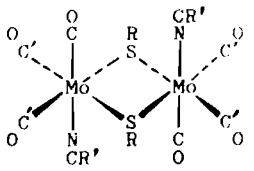

3 (C_{2h})

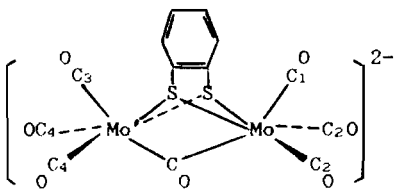

4 (C_s)

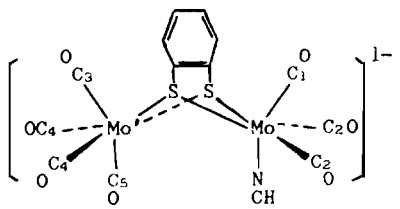

5 (C_s)

TABLE 1. Percentage d–d orbital components of the fragment $(CO)_4Mo–Mo(CO)_4$

MO	Orbital energy (eV)	Mo								
		s	p_x	p_y	p_z	$d_{x^2-y^2}$	d_{z^2}	d_{xy}	d_{xz}	d_{yz}
b_{3g}	−9.94			6.7						15.6
$2a_g$	−10.05	3.3			8.3	2.6	6.9			
b_{2u}	−10.07			7.6						17.0
b_{1u}	−11.48	0.5				12.6	15.1			
$1a_g$	−11.53					11.2	18.4			
a_u	−11.69							28.4		
b_{1g}	−11.71							28.4		
b_{2g}	−11.72								27.4	
b_{3u}	−11.85								27.5	

TABLE 2. Percentage orbital components of the frontier orbitals of the complex $[(CO)_4Mo(SH)_2Mo(CO)_4]^{2-}$

MO	Orbital energy (eV)	Mo	S	2C	2C′	2O	2O′	Bonding character
		4d	3p	2p	2p	2p	2p	
$2b_{1u}$	−9.032		1.7	36.7	1.1	9.4		
b_{3g}	−9.070		1.9	37.2		9.7		
$1b_{1u}$[a]	−11.221	26.3	2.1		14.0		6.9	σ^a
$2b_{3u}$	−11.275	19.5	10.2	8.3	5.4	4.0	2.7	π
b_{1g}	−11.319	22.6	7.3	8.2	5.2	2.6	4.1	δ
a_g	−11.517	28.8			13.2		7.3	σ
a_u	−11.694	28.4		9.1	4.4	5.5	2.6	δ^a
b_{2g}	−11.719	27.4		8.7	5.4	5.2	3.3	π^a
$1b_{3u}$	−13.344	6.3	29.3	4.9		6.6	1.6	

[a]Denotes the HOMO.

teraction with the corresponding symmetrically-adopted bridging S 3p orbitals. Therefore the bonding and antibonding MOs co-exist between Mo atoms in **1**, indicative of the virtual non-bonding Mo–Mo interaction that is consistent with the Mo–Mo distance [4].

$(CO)_4Mo(\mu\text{-}SH)_2Mo(CO)_4$ (2)

Complex **2** is neutral in which both the Mo–Mo distance (2.939 Å) and the Mo–S_b bond length (2.449 Å) are shorter than their counterparts in complex **1** (Mo–Mo: 3.939 Å; Mo–S_b: 2.587 Å). The orbital components and bonding characters of **2** are listed in Table 3. A comparison of the MOs of complexes **1** and **2** (Tables 2 and 3) shows that the orbitals b_{1u}, b_{1g} and b_{2g}, especially b_{1u}, rise, while b_{3u}, a_g and a_u fall relatively.

The dianion **1** is able to undergo two-electron oxidation [2]. In the redox process, the formal oxidation state of the Mo center changed between 0 and +1. The bonding character of the frontier MOs of **2** suggests that the shortening of the Mo–Mo distance is favorable to destabilize the antibonding

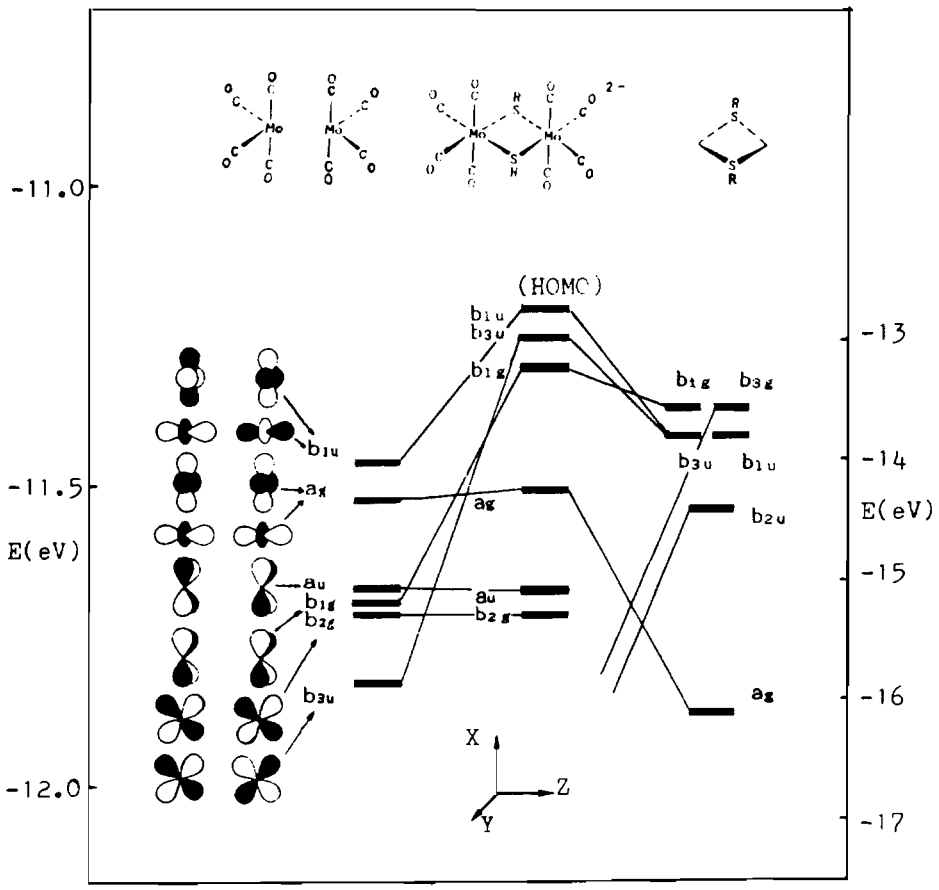

Fig. 1. Energy level correlation diagram for $[Mo_2(\mu\text{-}SH)_2(CO)_8]^{2-}$.

TABLE 3. Percentage orbital components of the frontier orbitals of the complex $(CO)_4Mo(SH)_2Mo(CO)_4$

MO	Orbital energy (eV)	Mo 4d	S 3p	2C 2p	2C' 2p	2O 2p	2O' 2p	Bonding character
b_{3g}	−9.107	1.1		36.6		9.3		
$2a_g$	−9.376			37.7		10.7		
b_{1u}	−9.421	22.2	12.4	1.4	10.6		2.6	σ^a
b_{1g}[a]	−10.976	17.8	11.9	7.4	7.0	3.1	3.0	δ
b_{2g}	−11.129	29.1		9.6	5.0	4.1	2.3	π^a
$2b_{3u}$	−11.496	19.7	10.8	8.8	3.8	4.8	2.1	π
$1a_g$	−11.633	35.4			8.7		4.9	σ
a_u	−11.713	27.1		8.2	6.3	4.8	3.7	δ^a
$1b_{3u}$	−13.103	7.4	28.7	5.9		6.2		

[a]Denotes the HOMO.

orbitals, b_{1u} (σ^*) and b_{2g} (π^*), and to stabilize the bonding orbitals, b_{3u} (π) and a_g. However, the shortening of the Mo–Mo distance has only a small effect on the δ bonding orbitals, b_{1g} and a_u, thus the five d-based orbitals b_{1g}, b_{2g}, b_{3u}, a_g and a_u, are occupied, and the orbital b_{1u} (σ^*) is unoccupied (LUMO). On account of the mutual cancellation of the π bonding and antibonding interactions between Mo atoms, only a σ bonding interaction in the orbital a_g exists, as expected from the electron counting.

$Mo_2(\mu\text{-}SH)_2(CO)_6(NCH)_2$ (3)

In certain conditions the carbonyl groups in **2** can be substituted by a $NCCH_3$ ligand forming complex **3**, the structure of which is similar to **2** [6]. In order to examine the influence of different terminal ligands on the Mo–Mo and Mo–CO interactions, we have calculated the electronic structure of **3**. The atomic charges, Mulliken overlap population, related bond lengths and bond angles (S–Mo–S) are listed in Table 4. As shown in Table 4, it is found that the oxidation of **1** gave rise to evident variation of the atomic charges of Mo and S, and caused the decrease of the Mulliken bond order of the Mo–C bond, which makes the substitutions of the carbonyls by other ligand easier. The substitution of the carbonyls of **2** by the NCH group does not significantly change the geometry of **3**. However, the Mulliken bond orders of the Mo–Mo, Mo–S and Mo–C bonds are increased, especially those of the Mo–C bond which

TABLE 4. Atomic charge (q), Mulliken bond order (r), bond lengths and bond angles (S–Mo–S)

		1		2		3	
q	Mo	−0.142		0.225		0.233	
	S	−0.275		0.038		−0.121	
	C	0.617		0.622		0.428	
	C′	0.515		0.639		0.623	
	O	−0.716		−0.716		−0.820	
	O′	−0.771		−0.741		−0.688	
	N					−0.407	
	H	0.128		0.129		0.136	
r	Mo–Mo	−0.022	(3.939)[a]	0.100	(2.939)	0.101	(2.966)
	Mo–S	0.419	(2.587)	0.389	(2.449)	0.446	(2.461)
	Mo–C	0.823	(2.026)	0.806	(2.025)	0.931	(1.950)
	Mo–C′	0.828	(1.946)	0.758	(2.013)	0.761	(2.007)
	Mo–N					0.420	(2.230)
Bond angle (°)		80.80		106.23		105.90	

[a]Bond lengths (Å) are in parentheses.

increased by 15.5% in **2**, and the negative charges of the S and C atoms which increased by 0.159 and 0.194, respectively. This shows that complex **3** is more stable than **2**, and would be unlikely for further substitution of CO ligands.

Possible oxidation of 2

As mentioned above, the two-electron oxidation of **2** led to the decrease of the Mo–Mo distance by 1 Å and correspondingly changes the Mo–S–Mo angle from 80.8° (in **1**) to 106.23° (in **2**) (see Table 4), and the formal oxidation state of Mo changes from 0 to +1. Therefore the following question arises: whether it is possible for a two-electron oxidation on **2** to form $[Mo_2(CO)_8(SH)_2]^{2+}$, in which Mo(I) is changed to Mo(II). There is not yet any experimental report regarding this question. To explore the possible redox case, we investigated the variation tendency of MOs with the geometry changed from **1** to **2**. Taking **1** as a starting point, fixing the Mo–S distance, and allowing the S–Mo–S angle to vary (the D_{2h} symmetry is maintained through out the variation), we obtained the Walsh diagram of the six upper occupied orbitals (see Fig. 2). Although the rise and fall of all those orbitals in Fig. 2 does not appear to be very straightforward, we can still obtain an explicit result by treating this diagram in the manner of a symmetry–antisymmetry pair (S–A pair) or orbitals [9], and discuss the trend of average energy of each S–A pair. The six Mo d-based orbitals form just three S–A pairs (Fig. 2). The variations of Mulliken bond orders and atomic charges with increasing of the S–Mo–S angle are given in Table 5. The schematic representation of the frontier orbital

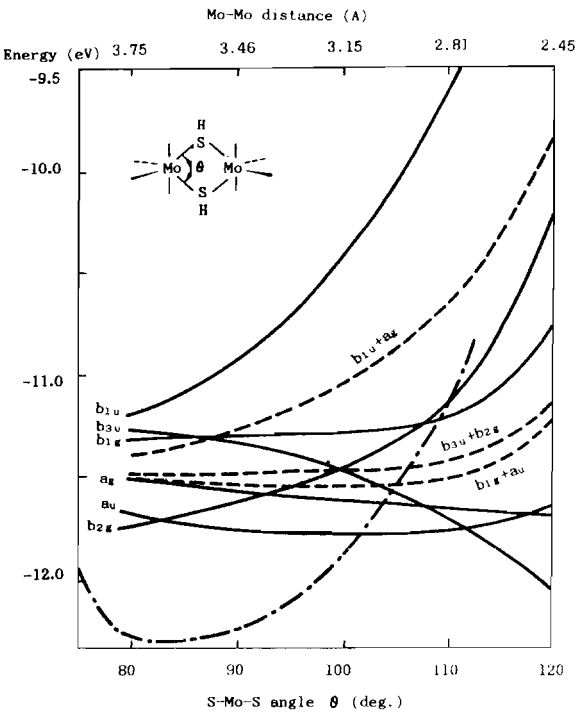

Fig. 2. Six d block levels of $[Mo_2(CO)_8(SH)_2]^{2-}$ as a function of S–Mo–S angle. A non-linear Mo–Mo distance scale is indicated on the top. Solid curve, d block levels; dashed curve, average energies of the symmetric–antisymmetric pair of orbitals; dashed-dot curve, total energy.

components of the complex $[Mo_2(\mu\text{-}SH)_2(CO)_8]^{2-}$ is given in Fig. 3.

The pairs a_u and b_{1g} maintain a fairly constant splitting as a function of the S–Mo–S angle, with a_u always located below b_{1g}, because there is no

TABLE 5. Variation of atomic charges and Mulliken bond order with increasing of the S–Mo–S angle in the complex $[Mo_2(CO)_8(SR)_2]^{2-}$

		S–Mo–S (°)				
		80	80.8	90	100	110
r	Mo–Mo	0.023	−0.023	0.029	0.024	0.018
	Mo–S	0.419	0.419	0.402	0.355	0.258
	Mo–C	0.823	0.823	0.822	0.824	0.828
	Mo–C′	0.826	0.828	0.842	0.844	0.832
q	Mo	−0.140	−0.142	−0.158	−0.171	−0.268
	S	−0.273	−0.275	−0.300	−0.326	−0.305
	C	0.617	0.617	0.619	0.619	0.621
	C′	0.514	0.515	0.517	0.531	0.577

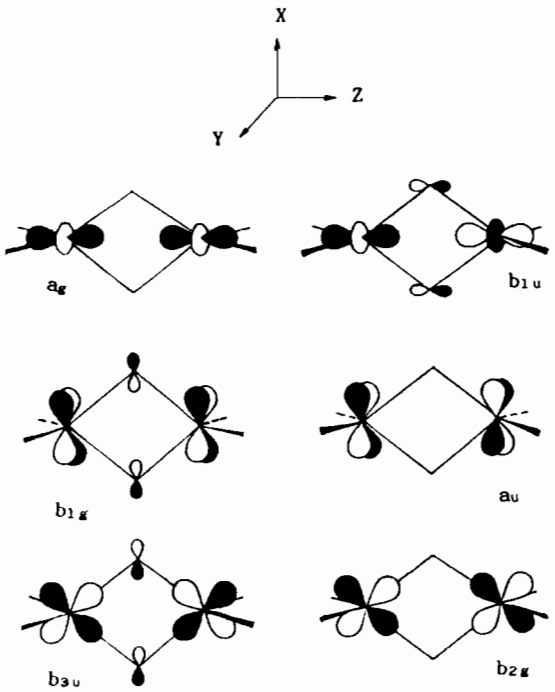

Fig. 3. Schematic drawing of frontier orbital components of $[Mo_2(CO)_8(SH)_2]^{2-}$.

symmetry matching between orbital a_u and bridging S orbitals. The orbital b_{1g} remains unchanged because of the non-bonding interaction with a sulfur p_x orbital. The through-space or direct Mo–Mo orbital interaction is of the δ type and not significant at a realistic metal–metal separation. The b_{3u}–b_{2g} pair starts at a small angle θ with b_{3u} laid above b_{2g}, because the sulfur p_x orbital destabilizes the b_{3u} combination. It should be noted that the b_{3u} orbital is the Mo–Mo π bonding and the b_{2g} orbital is π antibonding in character. As the S–Mo–S angle increases, the direct overlap between Mo atoms stabilizes b_{3u} and destabilizes b_{2g}. The two orbitals cross at about $\theta = 100°$. The through-space Mo–Mo interaction is of the σ type for the a_g–b_{1u} pair, which starts out at a long Mo–Mo distance with b_{1u} always laid above a_g. However, there is no symmetry matching between the orbital a_g and the bridging sulfur orbitals, and the sulfur p_z orbitals destabilize the b_{1u} combination, so that the orbital b_{1u} rises sharply as the S–Mo–S angle is increased. The ordering of the six orbitals in Fig. 2 at $\theta = 106°$ is in accord with that of **2** (see Table 2). Because of the energetically high-lying and antibonding HOMO (b_{1u}) for **1** at large Mo–Mo separation (see Fig. 2), it would be facile to lose two electrons, i.e. to undergo two-electron oxidation that turns **1** into more stable **2**. When the S–Mo–S angle is larger than 106°, the sum of the three pairs (dashed curves in Fig. 2) rise sharply, implying that the system is unstable. On the other hand, from the data listed in Table 5, it can be seen that as the S–Mo–S angle increases, the atomic charges on the Mo and S atoms are close to each other, and the Mulliken bond orders of the Mo–S bonds significantly decrease from 0.419 to 0.258, consequently the system is relatively unstable. The sharp rise of the total energy (dashed-dot curve in Fig. 2) with increasing of the S–Mo–S angle also verified this result. From Fig. 2, it can be seen that for **2** the HOMO (b_{1g}) is Mo–Mo bonding in character, so that further oxidation of **2** would be unlikely. Now we conclude that the oxidation state of the Mo(I) atoms in the complex $[Mo_2(CO)_8(SH)_2]$ (**2**) is difficult to increase by further oxidation, and that in the two-electron redox process the geometry of the system will 'resonate' between the structure of **1** and **2**.

$[Mo_2(CO)_7(S,S\text{-}C_6H_4\text{-}1,2)]^{2-}$ (4)

The structure of **4** is rather different from those of the three complexes containing the planar MoS_2Mo ring discussed above. Complex **4** possesses two thiolato and one carbonyl bridges with a Mo–Mo distance of 2.98 Å. The MoS_2Mo core in **4** adopts a 'butterfly' conformation in *syn–exo* geometry, and the two Mo–C(b) bond lengths are unequal. The MO calculations of **4** were carried out by taking the idealized C_s symmetry. The orbital components and bonding characters are listed in Table 6. The atomic charges and Mulliken bond orders are given in Table 7. Taking into account the orbital bonding characters of the frontier orbitals in Table 6, it can be shown that a very weak Mo–Mo interaction exists. In the cyclic voltammetry (CV) study, it was found that complex **4** underwent an irreversible one-electron oxidation reaction. Why irreversible? Upon study of

TABLE 6. Percentage orbital components and bonding characters of the complex $[Mo_2(CO)_7(S,S\text{-}C_6H_4\text{-}1,2)]^{2-}$

		MO					
		4a′	3a′	2a″	2a′	1a′	1a″
Orbital energy (eV)		−11.23	−11.33	−11.50	−11.57	−11.76	−11.89
Mo	sp					3.8	
	$d_{x^2-y^2}$	17.1	26.4			7.3	
	d_{z^2}	3.3			24.6		
	d_{xy}			9.7			16.3
	d_{xz}			12.9			10.0
	d_{yz}		11.5		9.8	3.5	
Mo′	$d_{x^2-y^2}$	18.6	2.1			19.9	
	d_{z^2}	2.0	8.8		13.8	13.6	
	d_{xy}			12.3			15.7
	d_{xz}			13.6			8.1
	d_{yz}	10.0	3.5				
C_b	p			3.3		15.5	6.2
S	p	5.2	5.6	2.4	6.4	1.0	2.2
Bonding character	Mo–Mo′	δ	δ^*, π^*	δ^*	σ	δ^*	δ, π
	C_b–Mo			π^*		σ	π
	C_b–Mo′			π		σ	π

[a]The HOMO.

TABLE 7. Atomic charges (q) and Mulliken bond order (r) of the complex $[Mo_2(CO)_7(S,S\text{-}C_6H_4\text{-}1,2)]^{2-}$

	Mo	Mo′	C_b	S	C_1	C_2	C_3	C_4
q	0.141	0.152	0.516	−0.203	0.455	0.458	0.688	0.528
	Mo–Mo′	Mo–S	Mo′–S	Mo–C_1	Mo–C_2	Mo′–C_3	Mo′–C_4	Mo′–C_b	Mo–C_b
r	0.096	0.399	0.391	0.912	0.923	0.735	0.855	0.715	0.205

the electronic structure of complex **4**, we suggest that under the influence of the solvent, $NCCH_3$, the weak Mo–CO carbonyl bridge would be cleaved and then the $NCCH_3$ group would coordinate onto the Mo′ center, based on the fact that the Mulliken bond order of the bridging Mo–CO bond (0.205) is much smaller than that of the Mo′–CO bond (0.715) (see Table 7). In this way, the oxidation turns the Mo(0) into Mo(I), and Mo′(0) remains unchanged. Thus the oxidation reaction would presumably lead to the formation of the proposed model complex $[Mo_2(CO)_7(NCCH_3)(S,S\text{–}C_6H_4\text{–}1,2)]^-$. In this study, we also calculated the electronic structure of the model complex $[Mo_2(CO)_7(NCH)(S,S\text{–}C_6H_4\text{–}1,2)]^-$ (**5**). In the calculation, the structural parameters of the fragments $Mo'(CO)_4$ and $Mo(CO)_3(NCH)$ in **5** were taken from the corresponding parts of complexes **1** and **3**. The coordination of the group NCH onto Mo destabilizes the system, causing the HOMO rises in energy of about 1.2 eV and the HOMO becomes markedly Mo–Mo $d\sigma^*$ antibonding in character. This fact indicates that the model complex **5** would more easily undergo electron loss, i.e. oxidation reaction. We propose that the cleavage of the Mo–CO bridging bond and the coordination of the solvent ligand NCH (actually $NCCH_3$) on the Mo center would be the reason why the CV oxidation is irreversible.

Acknowledgements

We are grateful to the National Natural Science Foundation of China and the Foundation of Chinese Academy of Sciences for grants in support of this work.

References

1 B. Zhuang, J. W. McDonald, F. A. Schultz and W. E. Newton, *Organometallics, 3* (1984) 943; *Inorg. chim. Acta, 99* (1985) L29.

2 B. Zhuang, L.-R. Huang, Y. Yang and J.-X. Lu, *Jiegou Huaxue (J. Struct. Chem.), 4* (1985) 103.

3 D. A. Smith, B. Zhuang, W. E. Newton, J. W. McDonald and F. A. Schultz, *Inorg. Chem., 26* (1987) 2524.

4 B. Zhuang, L.-R. Huang, L.-J. He, Y. Yang and J.-X. Lu, *Inorg. Chim. Acta, 145* (1988) 225.

5 B. Zhuang, L.-R. Huang, L.-J. He, Y. Yang and J.-X. Lu, *Inorg. Chim. Acta, 127* (1987) L7.

6 B. Zhuang, L.-R. Huang, Y. Yang and J.-X. Lu, *Inorg. Chim. Acta, 116* (1986) L41.

7 B. Zhuang, L.-R. Huang, L.-J. He and J.-X. Lu, *Inorg. Chim. Acta, 160* (1989) 229.

8 C.-W. Liu, J.-M. Hua, Z.-D. Chen, Z.-Y. Lin and J.-X. Lu, *Int. J. Quantum Chem., 29* (1986) 701.

9 R. H. Summerville and R. Hoffmann, *J. Am. Chem. Soc., 98* (1976) 7240.